Experimental research on the effect of the ball burnishing process, using new kinematical scheme on hardness and phase composition of surface layer of AISI 304L stainless steel

Diyan M. Dimitrov[1,*], *Stoyan* D. Slavov[2], and *Zhivko* Dimitrov[3]

[1]TU-Varna, Department of Mechanics and Machine Elements, 9010 Varna, Bulgaria
[2]TU-Varna, Department of Technology of Machine Tools and Manufacturing, 9010 Varna, Bulgaria
[3] HTP TU-Varna, 9010 Varna, Studentska 1 str., Bulgaria

Abstract. In this paper, experimental results about hardness and phase composition of surface layer of AISI 304L SS, machined by using ball burnishing process, conducted under a new kinematic scheme, are presented. The effect of different combinations of the process regime parameters on the amount of strain induced martensitic phase, is discussed. The amounts of austenitic and strain induced martensitic phases are identified by x-ray diffractometer. Micro hardness along the depth of the hardened layer is measured. Conclusions about the influence of the ball burnishing process on strain induced martensitic phase are given.

1 Introduction

Besides producing a specific surface finish (roughness with regular microshape), the ball burnishing process has additional advantages in comparison to other finishing processes, such as providing increased hardness, corrosion resistance and fatigue life, caused by compressive residual stress in the surface layer. Previously published works indicated that ball-burnished surfaces have many advantages in comparison with machined, milled or ground surfaces [1-5, 12]. In general, the regime parameters, affecting the plastic deformation process, are variable and they can include the burnishing speed, the burnishing feed, the burnishing compressive force as well as the number of passes of the burnishing tool over the same region of the processed surface. Thus, by appropriate adjustment of the regime parameters of ball burnishing process, it is possible to obtain compressive residual stresses in the surface region that could lead to considerable improvement in the component life.

Considering some known drawbacks of the classical kinematical schemes for implementation of vibrational ball-burnishing process, some new schemes are developed, based on the advantages of contemporary CNC machines [3]. In the process of ball burnishing, implemented under a new kinematical scheme, the ball tool also performs motion, following a complex trajectory. In this case, however, the tool path is obtained by means of a linear (or circular) interpolation, using the pre-calculated in a suitable CAD (or

* Corresponding author: dimitrov.diyan@gmail.com

CAM) software curve (polyline) [3], and not by compelled oscillations as in the classical scheme of the process. Furthermore, using CNC machines, some other parameters of burnishing process, such as feedrate can be changed steplessly and more widely, allowing far more precise adjustments of the processing.

In most of the austenitic stainless steel grades strain hardening effect is combined with a phase transformation. The formation and the amount of strain-induced martensite depends on the austenite stability (the chemical composition and the initial austenite grain size) and the strain hardening conditions (the deformation temperature, strain and strain rate) [6, 7].

The main objective of the current research is to investigate the correlation between phase composition of the hardened layer, obtained by a ball burnishing process under a new kinematic scheme and fatigue life of stainless steel grade 304L.

2 Experimental

2.1 Material and specimen preparation

Beam like specimens with a hemispherical stress concentrator, Fig.1.a, are laser cut of stainless steel grade ASTM 304L (Cr18Ni8) sheet with a thickness of 4 mm. The chemical composition of the steel is given in Table 1.

Table 1. Chemical composition of the steel grade ASTM 304L (Cr18Ni8).

C, %	Si, %	Mn, %	P, %	S, %	Cr, %	Ni, %	N, %
0.021	0.38	1.55	0.031	< 0.001	18.2	8.1	0,059

Before cutting, on both sides of the plate in rectangular bands with a width of 10 and a length of 40 mm regular relief (RR) by a ball burnishing under a new scheme, are formed.The regimes of the ball burnishing process are chosen, following four factors, full factorial experiment design with two levels per factor [1]. A low and a high level of each factor are given in tabl.2, where: **F [N]**-the external force on the ball tool; **i**– number of the sinusoids within the length of the toolpath, determining the parameter $(\pi \cdot D)/i$,[mm], related to the height of the obtained RR cells; **e [mm]**–half of the amplitude of the sine wave, related to the width of the obtained RR cells; **s [mm/min]** – feeding speed of the ball tool, following the sinusoidal trajectory.

Table 2. Regime parameters of the ball burnishing process.

Level	Regime parameters			
	F, N	I	e, mm	s, mm/min
Low	1865	600.15	1	150
High	3040	1200.15	2.5	300

2.2 Vibration fatigue resonance test

For the fatigue life test, the specimens are positioned on a shaker as a cantilever beam with a mounted accelerometer at the tip end, Fig.1.b. The accelerometer acts as a measuring device and a tip mass.

Tests are carried out at a frequency, equal to the first resonance frequency of a cantilever, which is ~90Hz.

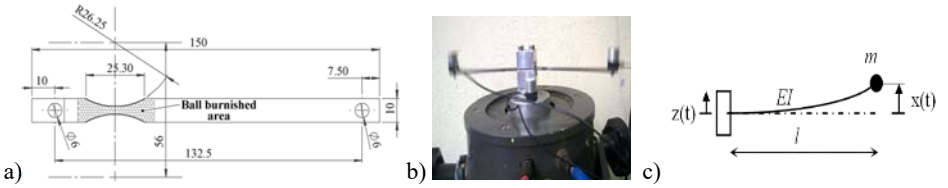

a) b) c)

Fig. 1. a) Configuration and dimensions of the experimental specimens; b) Positioning of the specimens on the shaker; c) Equivalent dynamics model.

The loading amplitude is kept equal for all tests. Two specimens are tested simultaneously to shorten the experimental time. Detailed explanation of vibration test is given in [1].

2.3 Phase composition and metallography analysis

The phase composition of the surface layer is studied with an X-rays diffractometer (XRD) with Brag-Brentano geometry in Cr-Kα radiation. According to the rolling direction longitudinal and transversal sections are cut, polished and etched from some of the specimens for metallography analysis. A light optical microscope Neophot 32 is used. A microhardness Vickers test is carried out with a 50g loading to measure the depth of the hardened layer.

3 Results and discussion

The X-ray diffractogram of the row material shows only the austenite γ peaks. In the ball burnished specimens, peaks of strain induced α' martensite also appears. Since in some diffractograms only α'(110) peak is clear, as an indicator for strain hardening effect after a ball burnishing, ratio "r" between intensities of α'(110) and γ(111) diffraction peaks, is used. According to this ratio the structures are divided into 5 groups. The typical diffraction patterns for each group are given in Fig. 2.

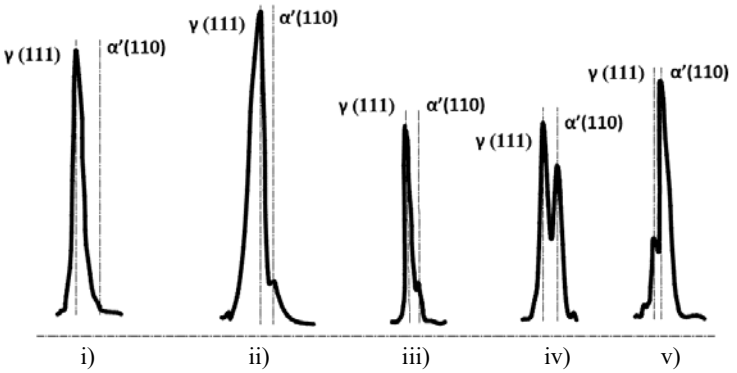

Fig. 2. Typical X-ray diffraction for γ(111) - 2θ=67.5° α'(110) - 2θ=69.5° each structural group i) r=0 ii) r=0.03-0.10 iii) r=0.12-0.25 iv) r=0.50-1.00 v) r>2.

The first group is characterised with no α'(110) peak r=0. The austenite γ(111) peak is broadened with a high intensity. The second group is characterised with a small α'(110) peak, partly hindered from broad γ(111) peak r=0.03-0.10. The third group is characterised with a more clear weak intensity α'(110) peak r=0.12-0.25. The next group is characterised by similar intensities of the two peaks r=0.5-1.00. And the last group is characterised with a strong α'(110) peak r>2.

Such scattering of the phase composition can be explained with a particular chemical composition of the raw material. On the base of the chemical composition, given in tabl.1 temperature M_{d30} =13,75°C (temperature at which 50% of A is transformed to M under 30% true strain) is calculated. As stated in [8] at such high value of M_{d30} austenite phase is very unstable. Authors in [9] shows X-ray difractogram after a deep rolling of 304L steel, which according to α'(110)/ γ(111) ratio can be classified in group (iv), and estimated the martensitic volume fraction on 27,5%. Similar results are obtained from Altenberger and all [10] after deep rolling.

The registered cycles to failure from fatigue test of specimens from each structure group are shown on Fig. 4 and a summary statistic of each group (mean and coefficient of variation CV) is presented in Table.3.

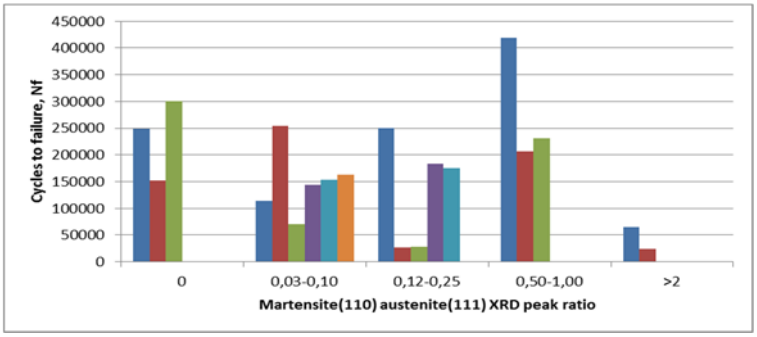

Fig. 3. Cycles to failure of specimens fall in each structural group.

Table 3. Summary statistic of specimens in each group from Fig.3.

M/A peak ratio "r"	0	0,03-0,10	0,12-0,25	0,50-1,00	>2
mean	233802	149794	132647	285598	44156
CV, %	32	41	76	41	65

It can be seen that the fourth (r=0.5-1.0) structure group give the highest mean fatigue life and the fifth group with r>2 gives a very short fatigue life, similar to non-plastically deformed specimens, which is about 20000 cycles [1]. As a general rule, the fatigue life increases with the increase of the martensite content in the volume but, as it is mentioned in [11], at 54 vol-% martensite more brittle behaviour and higher notch sensitivity of the martensite phase become predominant and lead to crack initiation at inclusions in the very high cycle fatigue (VHCF) regime. The fatigue tests of predeformed specimens with martensite content up to 36%, made in [8] show optimum for martensite volume fraction below 26%.

In the third group (r=0.12-0.25) there are two specimens with a short fatigue life, similar to those in r>2 group. We suppose that fatigue life of these specimens is affected by other factors (random micro stress concentrators or inclusions), which have to be additionally investigated on broken surfaces.

3.2 Hardness and microstructure

The surface hardness of all specimens increases with about 50% from 180HV10 of raw sheet to 260-280HV10 on plastically deformed surfaces. For a microstructure analysis two specimens, coded as "5" and "15" are chosen. These specimens fall in the third structural group. The regime parameters of the ball burnishing process differ only in parameter "i". It has a low value for specimen 5 (N_f=*182826*) and a high value for specimen 15(N_f=*250202*), tabl.2. A higher value of "i" means that the burnishing tool passes over the same region more

frequently. Other parameters of the regime are F=3040N, e=1 mm; s=150mm/min. The microstructures in the near surface area, presented on Fig. 4 and 5, are similar.

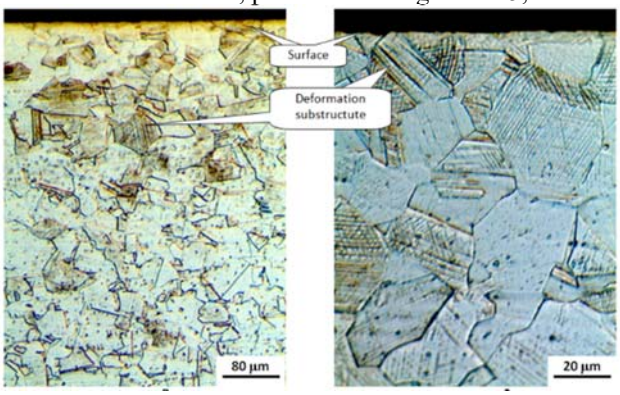

Fig. 4. Microstructures of specimen "5" near the surface.

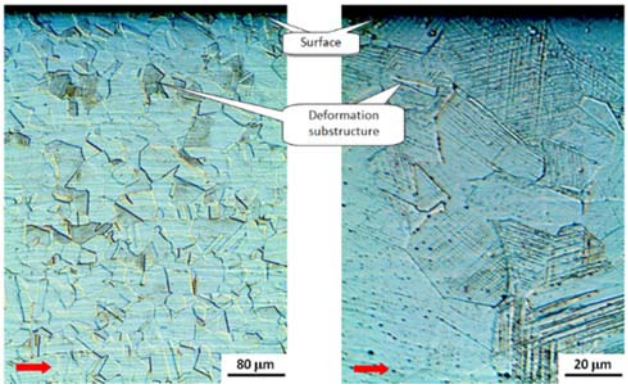

Fig. 5. Microstructures of specimen "15" near the surface (red arrow –rolling direction).

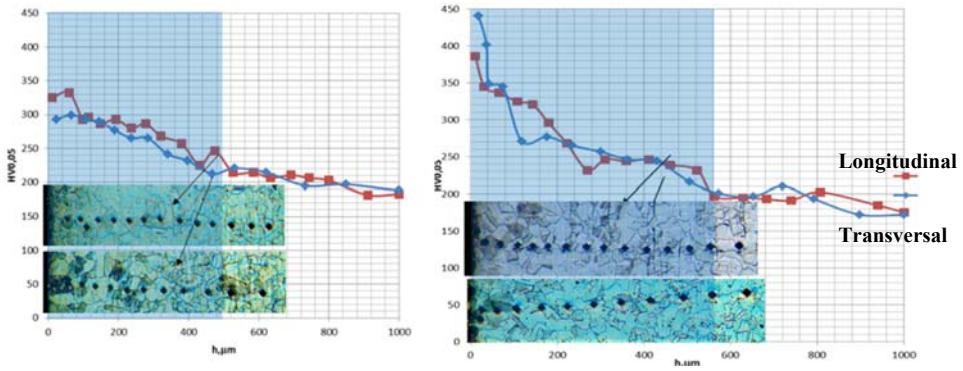

Fig. 6. Microhardness profile in depth of the deformed layer (left -5; right -15).

The deformation substructure with martensite needles, crossing each other in some of the austenitic grains, is clearly visible. The microhardness measurements, Fig. 6, show that the depth of the hardened layer in both specimens is about 500µm, but in specimen "15" higher hardness values are measured close to the surface, which results in slightly higher fatigue life.

4 Conclusion

On specimens from sheet stainless steel 304L grade, a hardened layer with a depth of about 500μm was obtained by ball burnishing process under a new kinematic scheme. Obviously, the fatigue life is extended but careful control on regime parameters of burnishing is needed, since the austenite phase in 304L steel is unstable and sensitive to the particular chemical composition of the alloy, different amounts of strain induced martensite are registered. As a result from the experiment, it is evident that there is a threshold value of the amount of martensite content, beyond which the fatigue life drastically shortens. It can be recommended to use a low level of the loading force, combined with high values of "i", which guaranties that the burnishing tool passes over the same region more frequently and obtaining near surface sublayer with a high hardness.

Our future work will be focused on investigation on the influence of the regime parameters of the ball-burnishing process on operating characteristics and phase composition for different grades of austenitic stainless steels, like 316L for example.

References

1. S.D. Slavov, D.M. Dimitrov. ECУ. **4-2 (25),** 11-22 (2016)
2. L. G. Odintsov, Hardening and Finishing of Parts by Surface Plastic Deformation. Mashinostroenie, Moscow (1987).
3. S. D. Slavov. International virtual journal "Machines, Technologies, Materials", **8,** 29-33 **(**2011)
4. Schneider Yu. G. Operational properties of parts with regular microrelief, publishing IVA, St. Petersburg, (2001)
5. I. Altenberger, Proceedings of 9th international conference on shot peening. IITT-International, 6-9, (2005)
6. J.Y. Choi, W. Jin,Scr. Mater., **36 (1)**, p. 99-104 (1997)
7. H Mirzadeh, A Najafizadeh Materials characterization **59 (11)**, 1650-1654 (2008)
8. Müller-Bollenhagen, C., Zimmermann, M., & Christ, H. J. Int. J. Fatigue, **32(6)**, 936-942. (2010)
9. J. Muñoz-Cubillos, J.J. Coronado, S.A. Rodríguez, , Int. J. Fatigue, **95** (2017), pp. 120–131
10. I. Altenberger, B. Scholtes, U. Martin, and H. Oettel, Mater. Sci. Eng. A, 1999, 264, p. 1–16
11. Müller-Bollenhagen, C., Zimmermann, M., & Christ, H. J. Procedia Engineering, **2(1)**, 1663-1672. (2010)
12. Amdouni, H., Bouzaiene, H., Montagne, A. et al. Int J Adv Manuf Technol (2016). doi: 10.1007/s00170-016-9529-9